Preparation of Highly Ordered Mesostructured Tin Oxide Film with a Microcrystalline Framework through Vapor-Induced Liquid-Crystal Templating

Hirokatsu Miyata,* Miki Itoh, Masatoshi Watanabe, and Takashi Noma

Core-Technology Development Headquarters Canon Research Center, Canon Inc., 5-1, Morinosato-Wakamiya, Atsugi-shi, Kanagawa, 243-0193 Japan

Received September 3, 2002. Revised Manuscript Received December 18, 2002

An optically transparent hexagonal mesostructured tin oxide film with a microcrystalline framework was prepared by combining dipcoating and a subsequent treatment with water vapor. After a substrate was coated with an alcoholic precursor solution containing tin tetrachloride and nonionic surfactant, the substrate was subject to a process to form a highly ordered mesostructured film on the substrate. Although the film after the simple drying process was opaque and showed only poor structural ordering, a short post-treatment with water vapor at low temperature significantly improved the transparency and the structural ordering of the film. It was proved that the longer low-temperature post-treatment induces the crystallization of the framework, preserving the ordered channel structure though vertical shrinkage of the periodic structure and degradation of the ordering were concomitantly observed. The post-treatment could not be replaced by the addition of water in the precursor solution. Though water was added to the system, the film was opaque and showed only poor structural ordering without the post-treatment. These results show that the present process cannot be a simple solvent evaporation process. It was shown that the formation of a lyotropic liquid-crystal phase induced by the exposure to water vapor before the completion of the condensation plays an essential role in the preparation process.

Introduction

Mesostructured materials prepared through self-assembly of surfactants attract worldwide attention as key materials for "bottom-up" styled nanotechnology in the 21st century. Since the discovery in 1990 by Yanagisawa et al.,[1] a wide variety of mesostructured materials[2−4] with different preparation,[5−8] composition,[9−14] andmorphology[15−23] have been reported. In particular, films of mesostructured materials[24−30] are promising for optical and electronic applications through incorporation

* To whom correspondence should be addressed. E-mail: miyata.hirokatsu@canon.co.jp.

(1) Yanagisawa, T.; Shimizu, T.; Kuroda, K.; Kato, C. *Bull. Chem. Soc. Jpn.* **1990**, *63*, 988.
(2) Ciesla, U.; Schüth, F. *Microporous Mesoporous Mater.* **1999**, *27*, 131.
(3) Ying, J. Y.; Mehnert, C. P.; Wong, M. S. *Angew. Chem., Int. Ed.* **1999**, *38*, 56.
(4) Schüth, F.; Schmidt, W. *Adv. Mater.* **2002**, *14*, 629.
(5) (a) Kresge, C. T.; Leonowicz, M. E.; Roth, W. J.; Vartuli, J. C.; Beck, J. S. *Nature* **1992**, *359*, 710. (b) Beck, J. S.; Vartuli, J. C.; Roth, W. J.; Leonowicz, M. E.; Kresge, C. T.; Schmitt, K. D.; Chu, C. T-W.; Olson, D. H.; Sheppard, E. W.; McCullen, S. B.; Higgins, J. B.; Schlenker, J. L. *J. Am. Chem. Soc.* **1992**, *114*, 10834.
(6) (a) Zhao, D.; Feng, J.; Huo, Q.; Melosh, N.; Fredrickson, G. H.; Chmelka, B. F.; Stucky, G. D. *Science* **1998**, *279*, 548. (b) Zhao, D.; Huo, Q.; Feng, J.; Chmelka, B. F.; Stucky, G. D. *J. Am. Chem. Soc.* **1998**, *120*, 6024.
(7) Attard, G. S.; Glyde, J. C.; Göltner, C. G. *Nature* **1995**, *378*, 366.
(8) Tanev, P. T.; Pinnavaia, T. J. *Science* **1995**, *267*, 865.
(9) (a) Huo, Q.; Margolese, D. I.; Ciesla, U.; Feng, P.; Gier, T. E.; Sieger, P.; Leon, R.; Petroff, P. M.; Schüth, F.; Stucky, G. D. *Nature* **1994**, *368*, 317. (b) Huo, Q.; Margolese, D. I.; Ciesla, U.; Demuth, G. D.; Feng, P.; Gier, T. E.; Sieger, P.; Firouzi, A.; Chmelka, B. F.; Schüth, F.; Stucky, G. D. *Chem. Mater.* **1994**, *6*, 1176.
(10) (a) Attard, G. S.; Bartlett, P. N.; Coleman, N. R. B.; Elliott, J. M.; Owen, J. R.; Wang, J. H. *Science* **1997**, *278*, 838. (b) Attard, G. S.; Göltner, C. G.; Corker, J. M.; Henke, S.; Templer, R. H. *Angew. Chem., Int. Ed. Engl.* **1997**, *36*, 1315.
(11) Antonelli, D. M.; Ying, J. Y. *Angew. Chem., Int. Ed. Engl.* **1996**, *35*, 426.
(12) Kimura, T.; Sugahara, Y.; Kuroda, K. *Chem. Mater.* **1999**, *11*, 508.
(13) (a) MacLachlan, M. J.; Coombs, N.; Ozin, G. A. *Nature* **1999**, *397*, 681. (b) MacLachlan, M. J.; Coombs, N.; Bedard, R. L.; White, S.; Thompson, L. K.; Ozin, G. A. *J. Am. Chem. Soc.* **1999**, *121*, 12005.
(14) (a) Inagaki, S.; Guan, S.; Fukushima, Y.; Ohsuna, T.; Terasaki, O. *J. Am. Chem. Soc.* **1999**, *121*, 9611. (b) Inagaki, S.; Guan, S.; Ohsuna, T.; Terasaki, O. *Nature* **2002**, *416*, 304.
(15) Yang, H.; Vovk, G.; Coombs, N.; Sokolov, I.; Ozin, G. A. *J. Mater. Chem.* **1998**, *8*, 743.
(16) Huo, Q.; Feng, J.; Schüth, F.; Stucky, G. D. *Chem. Mater.* **1997**, *9*, 14.
(17) (a) Grün, M.; Lauer, I.; Unger, K. K. *Adv. Mater.* **1997**, *9*, 254. (b) Grün, M.; Unger, K. K.; Matsumoto, A.; Tsutsumi, K. *Microporous Mesoporous Mater.* **1999**, *27*, 207.
(18) Lu, Y.; Fan, H.; Stump, A.; Ward, T. L.; Rieker, T.; Brinker, C. J. *Nature* **1999**, *398*, 223.
(19) Yang, P.; Zhao, D.; Chmelka, B. F.; Stucky, G. D. *Chem. Mater.* **1998**, *10*, 2033.
(20) (a) Marlow, F.; Spliethoff, B.; Tesche, B.; Zhao, D. *Adv. Mater.* **2000**, *12*, 961. (b) Kleitz, F.; Marlow, F.; Stucky, G. D.; Schüth, F. *Chem. Mater.* **2001**, *13*, 3587.
(21) Miyata, H.; Kuroda, K. *Adv. Mater.* **2001**, *13*, 558.
(22) (a) Melosh, N. A.; Lipic, P.; Bates, F. S.; Wudl, F.; Stucky, G. D.; Fredrickson, G. H.; Chmelka, B. F. *Macromolecules* **1999**, *32*, 4332. (b) Melosh, N. A.; Davidson, P.; Chmelka, B. F. *J. Am. Chem. Soc.* **2000**, *122*, 823.
(23) Feng, P.; Bu, X.; Stucky, G. D.; Pine, D. *J. Am. Chem. Soc.* **2000**, *122*, 994.
(24) Pevzner, S.; Regev, O.; Yerushalmi-Rozen, R. *Curr. Opin. Colloid Interface Sci.* **2000**, *4*, 420.
(25) Edler, K. J.; Roser, S. J. *Int. Rev. Phys. Chem.* **2001**, *20*, 387.
(26) (a) Ogawa, M. *J. Am. Chem. Soc.* **1994**, *116*, 7941. (b) Ogawa, M. *Chem. Commun.* **1996**, 1149.
(27) Lu, Y.; Ganguli, R.; Drewien, C. A.; Anderson, M. T.; Brinker, C. J.; Gong, W.; Guo, Y.; Soyez, H.; Dunn, B.; Huang, M. H.; Zink, J. I. *Nature* **1997**, *389*, 364.

10.1021/cm020870a CCC: $25.00
Published on Web 02/28/2003

of various guest species. Though some groups have reported the potential of mesoporous silica films for optical application,[31−33] development of mesostructured films of non-siliceous materials[34−36] with conductive or semiconducting properties is essential for expanding the field of possible application. Because many of the unique electronic properties of metal oxides emerge in the crystalline state, the crystallization of the pore wall in the films has been one of the major issues for these materials. Crystallization of the pore wall can be induced by high-temperature treatment. Yang et al. reported the formation of various mesoporous materials through the solvent evaporation method using triblock copolymers as structure-directing agents and showed the formation of microcrystals by calcination.[37] However, this high-temperature process for the crystallization is not always useful for the preparation of functional nanocomposite films.

Mesostructured materials are expected to be applied to functional materials by introducing various guest species into the mesopores. The strategies to incorporate guest species can be categorized into the following two: one is the strategy in which guest species are introduced into the hollow mesopores after the surfactant removal[33,38−40] and the other is to form the objective nanocomposites directly from the reactant solutions that contain guest species.[31,32,40−43] The recently reported strategy in which functional mesostructured materials are directly prepared using surfactants with functional groups[44−46] is also included in the second strategy. The first strategy is unfavorable, especially for films, not only because of degradation of the ordered structure during the processes of surfactant removal and guest incorporation but also because of difficulties in incorporating polymers or large molecules. The second strategy is more attractive from the viewpoint of self-organization research because it is based on skillful chemistry that was adopted by nature to create biomaterials. Again, the second strategy is industrially more useful because of easier implementation of the process. For these reasons, a low-temperature crystallization process of the wall-consisting materials is desired for the preparation of functional nanocomposites based on conductive or semiconducting non-siliceous mesostructured materials.

Among the various metal oxide materials, tin oxide is one of the most useful materials because of its electronic conductivity. Several groups have reported the formation of mesostructured tin oxide.[37,47−50] Yang et al. prepared a film through the combination of dipcoating and the subsequent aging process using a triblock copolymer,[37] but there is no detailed description about the aging process that is indispensable for the development of ordered mesostructures and the resultant film has relatively poor ordering with a thick pore wall. They reported the formation of cassiterite microcrystals in the pore wall during calcination. However, the coincidence of ordered mesostructure and microcrystals is not satisfactorily presented. Pinnavaia and co-workers reported the preparation of mesostructured tin oxide containing microcrystallites without calcination,[47] but only a powdered sample with poor structural ordering was obtainable.

In this paper, we report, for the first time, the low-temperature preparation of a transparent mesostructured tin oxide film with highly ordered hexagonal channel structure containing microcrystalline SnO_2 within the pore wall. After a substrate was coated with a precursor solution containing a nonionic surfactant and tin tetrachloride, it was dried once, and subsequently, it was subject to post-treatment with water vapor at low temperature. Although the simply dried film without the post-treatment was opaque and the ordering of the porous structure was very poor, short low-temperature treatment with water vapor incredibly enhanced the film continuity and the pore ordering. The post-treatment made the film completely transparent and brought a remarkable increase of the X-ray diffraction intensity. A transmission electron microscopic study proved the formation of a hexagonally packed channel structure over all the thicknesses in the film. Both the structure and the transparency of the film were independent of the water content in the precursor solution; that is, the highly ordered transparent mesostructured tin oxide film was not obtained without the post-treatment, even though a certain amount of water was added to the precursor solution. Although the longer post-treatment brought about vertical shrinkage and degradation of the mesostructure, it was proved that the crystallization of the pore wall concomitantly proceeded during the water vapor treatment without

(28) (a) Yang, H.; Kuperman, A.; Coombs, N.; Mamiche-Afara, S.; Ozin, G. A. *Nature* **1996**, *379*, 703. (b) Yang, H.; Coombs, N.; Sokolov, I.; Ozin, G. A. *Nature* **1996**, *381*, 589.
(29) Aksay, I. A.; Trau, M.; Manne, S.; Honma, I.; Yao, N.; Zhou, L.; Fenter, P.; Eisenberger, P. M.; Gruner, S. M. *Science* **1996**, *273*, 892.
(30) (a) Miyata, H.; Kuroda, K. *J. Am. Chem. Soc.* **1999**, *121*, 7621. (b) Miyata, H.; Kuroda, K. *Chem. Mater.* **2000**, *12*, 49. (c) Miyata, H.; Noma, T.; Watanabe, M. Kuroda, K. **2002**, *14*, 766.
(31) Yang, P.; Wirnsberger, G.; Huang, H. C.; Cordero, S. R.; McGehee, M. D.; Scott, B.; Deng, T.; Whitesides, G. M.; Chmelka, B. F.; Buratto, S. K.; Stucky, G. D. *Science* **2000**, *287*, 465.
(32) Wirnsberger, G.; Scott, B. J.; Chmelka, B. F.; Stucky, G. D. *Adv. Mater.* **2000**, *12*, 1450.
(33) Dag, Ö.; Ozin, G. A.; Yang, H.; Reber, C.; Bussière, G. *Adv. Mater.* **1999**, *11*, 474.
(34) Crepaldi, E. L.; Soler-Illia, G. J. A. A.; Grosso, D.; Albouy, P.-A.; Sanchez, C. *Chem. Commun.* **2001**, 1582.
(35) Grosso, D.; Soler-Illia, G. J. A. A.; Babonneau, F.; Sanchez, C.; Albouy, P.-A.; Brunet-Bruneau, A.; Balkenende, A. R. *Adv. Mater.* **2001**, *13*, 1085.
(36) Pidol, L.; Grosso, D.; Soler-Illia, G. J. A. A.; Crepaldi, E. L.; Sanchez, C.; Albouy, P.-A.; Amenitsch, H.; Euzen, P. *J. Mater. Chem.* **2002**, *12*, 557.
(37) (a) Yang, P.; Zhao, D.; Margolese, D. I.; Chmelka, B. F.; Stucky, G. D. *Nature* **1998**, *396*, 152. (b) Yang, P.; Zhao, D.; Margolese, D. I.; Chmelka, B. F.; Stucky, G. D. *Chem. Mater.* **1999**, *11*, 2813.
(38) Nguyen, T.-Q.; Wu, J.; Doan, V.; Schwartz, B. J.; Tolbert, S. H. *Science* **2000**, *288*, 652.
(39) Murata, S.; Furukawa, H.; Kuroda, K. *Chem. Mater.* **2001**, *13*, 2722.
(40) Ogawa, M.; Nakamura, T.; Mori, J.; Kuroda, K. *J. Phys. Chem. B* **2000**, *104*, 8554.
(41) Marlow, F.; McGehee, M. D.; Zhao, D.; Chmelka, B. F.; Stucky, G. D. *Adv. Mater.* **1999**, *11*, 632.
(42) Ogawa, M. *Langmuir* **1995**, *11*, 4639.
(43) Hernandez, R.; Franville, A.-C.; Minoofar, P.; Dunn, B.; Zink, J. I. *J. Am. Chem. Soc.* **2001**, *123*, 1248.
(44) Aida, T.; Tajima, K. *Angew. Chem., Int. Ed.* **2001**, *40*, 3803.
(45) Lu, Y.; Yang, Y.; Sellinger, A.; Lu, M.; Huang, J.; Fan, H.; Haddad, R.; Lopez, G.; Burns, A. R.; Sasaki, D. Y.; Shelnutt, J.; Brinker, C. J. *Nature* **2001**, *410*, 913.
(46) Ikegami, M.; Tajima, K.; Aida, T. *Abstr. 3rd Int. Mesostruct. Mater. Symp.* **2002**, 164.
(47) Severin, K. G.; Abdel-Fattah, T. M.; Pinnavaia, T. *Chem. Commun.* **1998**, 1471.
(48) Chen, F.; Liu, M. *Chem. Commun.* **1999**, 1829.
(49) Ulagappan, N.; Rao, C. N. R. *Chem. Commun.* **1996**, 1685.
(50) Qi, L.; Ma, J.; Cheng, H.; Zhao, Z. *Langmuir* **1998**, *14*, 2579.

structural collapse. The growth of the microcrystals in the pore wall tends to be limited, and the final crystal size, ~2.0 nm, was consistent with the wall thickness. The structural change of the film ceased when the exposure to water vapor was stopped, showing that both of the changes, in mesostructure and crystallization, are induced by moisture.

Experimental Section

Materials. A Corning non-alkaline glass plate (#7059) with a size of 25 × 38 mm and 1.0-mm thickness was used as a substrate. Anhydrous tin tetrachloride with 99.999% purity was purchased from Kojundo Chemical Laboratory Co. Poly(oxyethylene) alkyl ethers (nonionic surfactants), $C_{18}H_{37}(OCH_2CH_2)_{10}OH$ (abbreviated as $C_{18}EO_{10}$, commercial name Brij76) and $C_{16}H_{33}(OCH_2CH_2)_{20}OH$ (abbreviated as $C_{16}EO_{20}$, commercial name Brij58), were purchased from Aldrich Chemical Co. and used as received. Ethanol (EtOH) with >99.5% purity was supplied by Kishida Chemical Co. and used without further purification. Deionized water with the resistivity of >18 M Ωcm was used for the experiments.

Preparation of the Reactant Solution. $C_{18}EO_{10}$ was dissolved in EtOH or EtOH/H_2O mixed solvent with a ratio of 2.0 g of $C_{18}EO_{10}$ /20 g of solvents, and 0.022 mol of anhydrous tin tetrachloride ($SnCl_4$) was slowly added with vigorous stirring under a nitrogen gas atmosphere. The mixed solvent consists of 16.4 g of EtOH and 3.6 g of H_2O. $C_{16}EO_{20}$ was dissolved in deionized water with a ratio of 2.0 g of $C_{16}EO_{20}$/20 g of water, and 0.022 mol of $SnCl_4$ was slowly added with vigorous stirring under nitrogen. The solutions were used after cooling to ambient temperature.

Preparation of the Films. The substrates were coated with the above precursor solutions by dipcoating. The substrates were dipped into the solutions perpendicularly and were withdrawn with a speed of 2−7 mm/s. The substrates were transferred into a container that affords the control of temperature and relative humidity (RH) and were dried for 10 h under the conditions of 40 °C, 20% RH. Then the humidity in the container was continuously increased to 80% RH at a rate of 1%/min, and the films were exposed to water vapor for a given period. After the water vapor treatment, the humidity was continuously decreased to 20% RH with the rate of −1%/min. For the investigation of the structural change in short time scales, the film dried under 40 °C, 20% RH conditions was directly transferred into another container set at 40 °C, 80% RH and was kept there for a desired period.

Characterization. The structure of the films was elucidated by X-ray diffraction (XRD). Conventional $\theta-2\theta$ scanning XRD was performed with a Rigaku RAD-RC using Cu Kα radiation from a copper rotating anode under operating conditions of 40 kV, 40 mA using a nickel filter. To record the small-angle region, very narrow slits were employed; the divergence slit, the scattering slit, and the receiving slit was 1/6°, 1/6°, and 0.05 mm, respectively. The wide-angle diffraction pattern of the film was recorded with Philips X-pert Pro using Cu Kα radiation under operating conditions of 45 kV, 40 mA. An optical geometry for thin film measurements was employed to reduce the background level due to scattering by the substrate. In this geometry, the incident angle was set to 0.5°, and an X-ray mirror with a divergence angle of 0.04° was used to obtain a parallel beam. A soller slit with a vertical divergence of 0.27° was set before the detector. A grazing angle (the incident angle of X-rays was 0.3°) in-plane XRD study[51] was performed to analyze the mesochannel orientation using an X-ray diffractometer equipped with a 4-axes goniometer (Rigaku ATX-G) with a parabolic multilayer mirror as a primary beam condenser. Cu Kα radiation from a copper rotating anode was used for the experiment, and a soller slit with a vertical divergence of 0.48° was used to obtain a parallel beam. The morphology of the samples was observed using an optical microscope (Olympus BX50) and a field emission scanning electron microscope (FE-SEM) (Philips XL-30) operating at an accelerating voltage of 3 kV. The images of transmission electron microscopy (TEM) and the electron diffraction pattern were recorded on a Hitachi H-800 at an accelerating voltage of 200 kV. The image of scanning transmission electron microscopy (STEM) was recorded on a Philips Tecnai F30 microscope at an accelerating voltage of 300 kV. The details of the preparation of the specimen for the cross-sectional TEM are described in a previous paper.[30b]

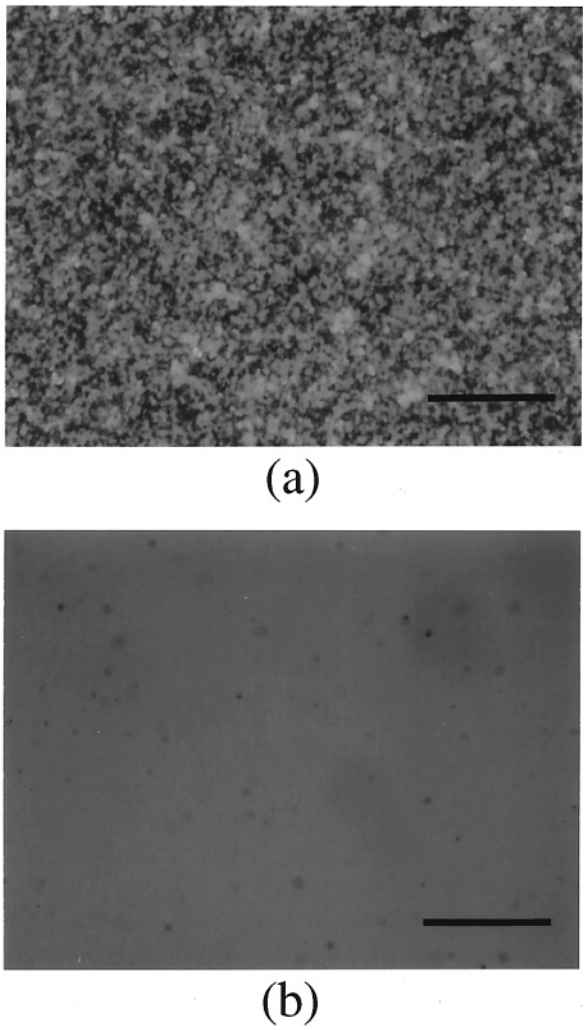

Figure 1. Optical micrographs of the mesostructured films (a) without the water vapor post-treatment and (b) after the water vapor post-treatment. Scale bar: 20 μm.

Results

Preparation of the Films with Ordered Mesostructure. The film simply dried for 10 h under the 40 °C, 20% RH conditions was opaque and granulated. The optical micrograph of the film is shown in Figure 1a. The $\theta-2\theta$ scanning XRD pattern of the dried film is shown as trace (a) in Figure 2. A weak broad diffraction peak corresponding to a lattice distance of 6.5 nm was observed. Although the film may have some structural ordering, judging from the broad peak, the order is quite low. As long as it was kept in such dry conditions, that is, under low humidity, the film remained opaque and the observed broad diffraction peak was almost unchanged.

However, when the relative humidity in the container was increased to 80% by introducing water vapor,

(51) Marra, W. C.; Eisenberger, P.; Cho, A. Y. *J. Appl. Phys.* **1979**, *50*, 6927.

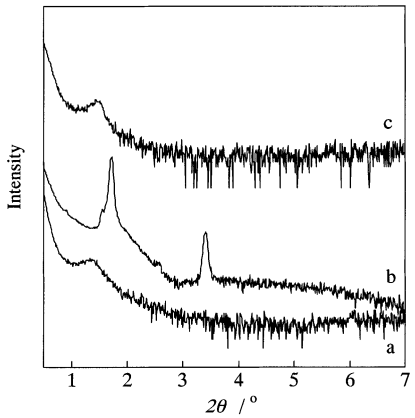

Figure 2. $\theta-2\theta$ XRD patterns of the mesostructured films (a) without the water vapor post-treatment, (b) after the 5-h post-treatment, and (c) after the 10-s post-treatment. The vertical axis is shown in a log scale.

keeping the temperature at 40 °C, the opaque film after the above drying process turned transparent (Figure 1b) and sharp diffraction peaks appeared instead of the broad peak. The diffraction intensity was more than 300 times that of the simply dried film. The XRD profile of the film that was kept under the high-humidity condition for 5 h is shown as trace (b) in Figure 2. Two diffraction peaks corresponding to lattice distances of 5.0 and 2.6 nm were observed in the pattern. The intense diffraction peaks indicate the formation of a highly ordered mesostructure.

For film samples of mesostructured materials, it is difficult to distinguish a two-dimensional hexagonal structure from a lamellar structure only by a $\theta-2\theta$ scanning XRD profile. Because hexagonally packed mesochannels in a mesostructured film run parallel to the substrate surface, both hexagonal and lamellar structures provide only (h00) peaks in their diffraction profiles. In such cases, in-plane XRD, which provides structural information on lattice planes perpendicular to the substrate, can be effectively used to confirm the structure. In the in-plane XRD pattern, a strong diffraction peak indexed as ($1\bar{1}0$) of a hexagonal structure[30c] was observed at a position corresponding to a lattice distance of 7.6 nm (see Supporting Information). Consequently, the possibility of formation of a lamellar structure was excluded. Therefore, the observed diffraction peaks were indexed as (100) and (200) of a hexagonal structure. This was proved by TEM observations, as will be shown later.

The uniformity and the transparency of the mesostructured film were considerably affected by the drying process. When the wet film immediately after the dip-coating was directly introduced into the high-humidity atmosphere, the prepared film was not uniform and was partially opaque. In this study, the relative humidity during the water vapor post-treatment was set to 80%. However, when the relative humidity for the posttreatment approached ~100%, the resultant film became opaque and highly uneven.

The mesostructure thus formed was independent of the film thickness within the experimental conditions. The films with different thicknesses, 1.5, 1.0, and 0.7 μm, were prepared by changing the coating speed, but the observed mesostructure was identical. However, the film uniformity was slightly affected by the film thickness, and thinner films tend to show superior uniformity.

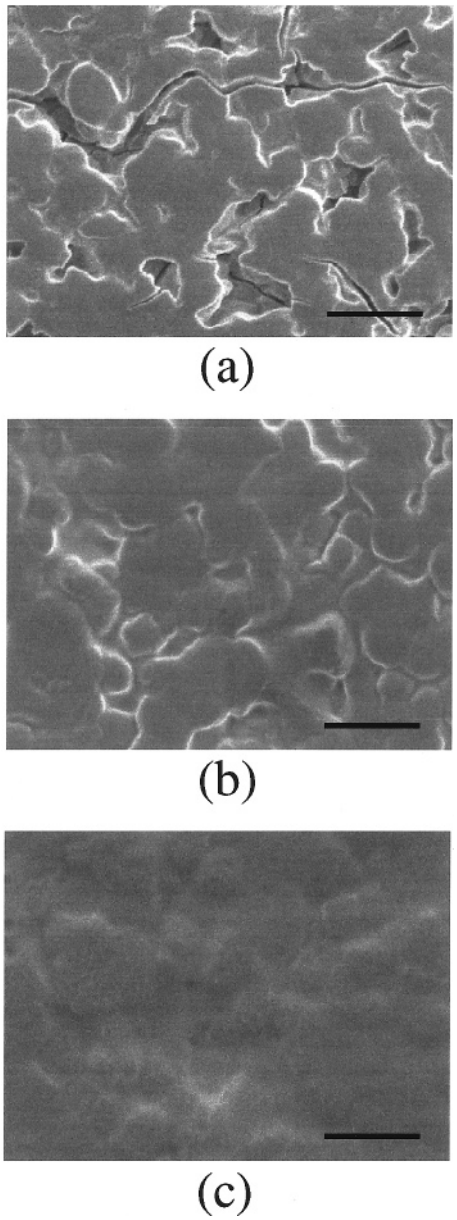

Figure 3. Change of the SEM images during the water vapor post-treatment. (a) Before the post-treatment and (b) after the 2-s post-treatment, relatively opaque part; (c) after the 2-s post-treatment, relatively transparent part. Scale bar: 2 μm.

From optical and electron microscopy, it was shown that the transparent film formation by the water vapor post-treatment accompanies a remarkable morphological change of the film. This morphological change proceeds rapidly and a film transparent to the eye was formed within only 10 s of post-treatment under the 40 °C, 80% RH conditions. A rapid morphological change has been shown by Crepaldi et al. for ZrO_2.[34] The morphological change in the present film was demonstrated using SEM as shown in Figure 3. Though the film is not continuous and consists of grains when it is dried in a 40 °C, 20% RH atmosphere (Figure 3a), the short (~2 s) water vapor post-treatment rapidly brings the connection of the grains (Figure 3b,c), leading to the formation of a continuous film. The surface of the film after the ~5-s post-treatment was completely flat and featureless within the present resolution of SEM. How-

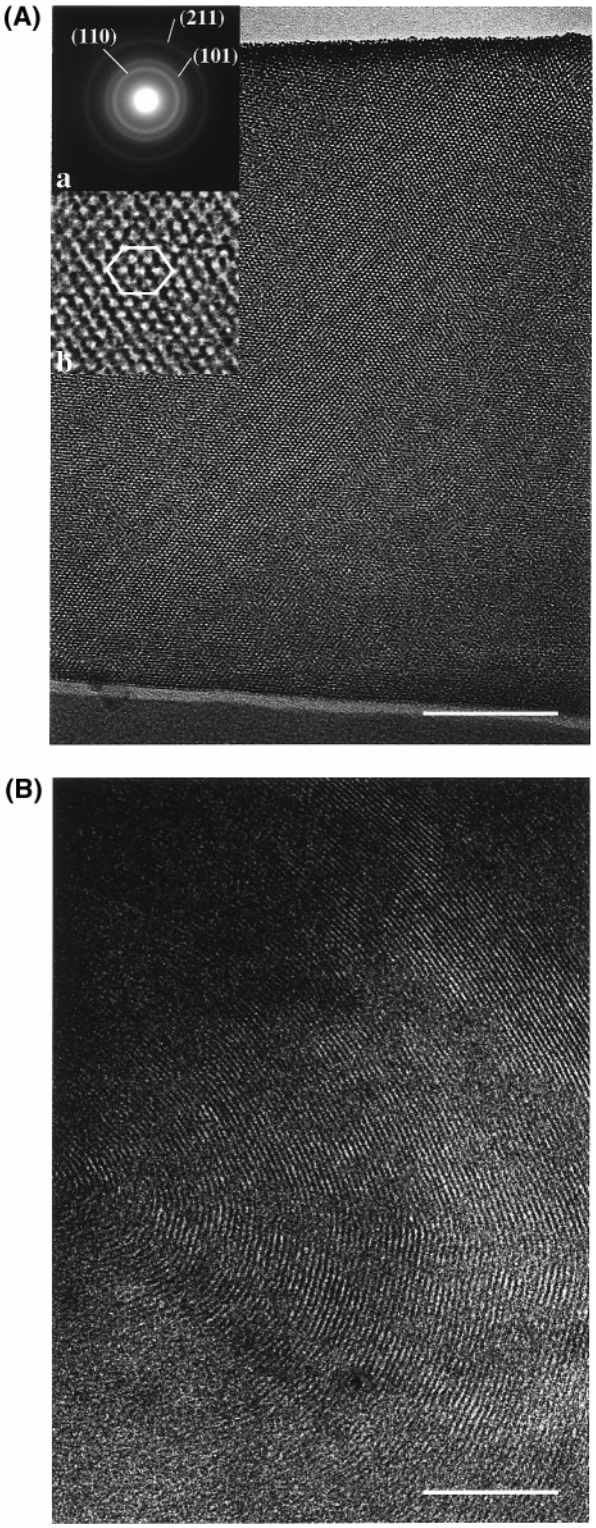

Figure 4. (A) Cross-sectional TEM image of the mesostructured tin oxide film. Inset (a): electron beam diffraction pattern recorded for the same area. Inset (b): high-magnification image of the mesostructured tin oxide film. (B) Top view TEM image of the mesostructured tin oxide film. Scale bar: 200 nm.

ever, the transparent film after the short (10 s) water vapor treatment does not give the sharp XRD peak (Figure 2, trace (c)), showing the ordered structure is not formed yet at this stage.

TEM Observations. The highly ordered structure of the mesostructured film prepared through dipcoating and the subsequent water vapor post-treatment was confirmed by TEM. Figure 4 shows the (A) cross-sectional image and (B) top view of the mesostructured film after the water vapor post-treatment. The hexagonal channel arrangement was observed for all the thicknesses of the film, confirming the formation of the hexagonal channel structure inferred from the XRD patterns. The mesochannels in the film run parallel to the substrate surface as shown in Figure 4A, but the curved or swirling stripes in the top view image of the film, Figure 4B, prove that the in-plane orientation of the mesochannels is random. The high-magnification cross-sectional TEM image (Figure 4A, inset (b)) shows that the vertical distance of the periodic structure is selectively shorter than the other two directions. This distortion in the hexagonal structure is likely to be caused by the anisotropic shrinkage of the pore wall through the condensation reaction.[30,34,35]

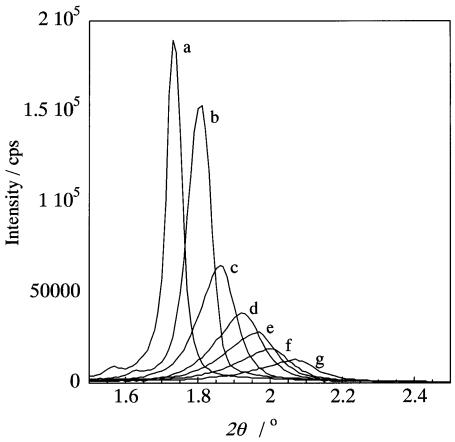

Figure 5. Change of the low-angle-region XRD pattern with the time of the water vapor post-treatment: (a) 5 h; (b) 20 h; (c) 50 h; (d) 80 h; (e) 120 h; (f) 220 h; (g) 320 h.

To estimate the pore wall thickness, an STEM image was recorded (not shown). Although the pore wall thickness of mesostructured materials estimated from TEM images is strongly affected by a small change of the focus, STEM images, which are based on the contrast by different elements, are independent of the focus. Therefore, STEM allows confident estimation of the thickness of the pore wall. The wall thickness of the present sample was estimated to be ~3.6 nm.

Crystallization of the Pore Wall. As described above, the post-treatment with water vapor caused the formation of a highly ordered mesostructure. The detailed profile of the (100) peak in the XRD pattern recorded for the film after 5 h of post-treatment is shown as trace (a) in Figure 5. The (100) peak after the 5-h post-treatment was very sharp and strong. The full width at half-maximum (fwhm) of the (100) peak was ~0.05°, which is narrower than that observed for the highly aligned hexagonal mesostructured silica film in our previous report.[30] This proves remarkably high structural ordering in the film. The wide-angle diffraction pattern ($2\theta = 20°-60°$) of the same film recorded with parallel beam optical geometry is shown as trace (a) in Figure 6. No substantial diffraction peak was observed except the sharp diffraction peaks at $2\theta = 38°$ and 44°, which are caused by aluminum used in the sample holder. It was shown that the 5-h post-treatment

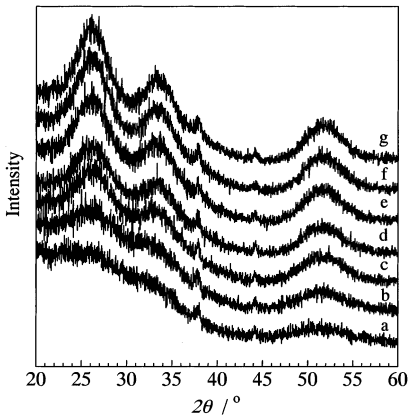

Figure 6. Change of the wide-angle-region XRD pattern with the time of the water vapor post-treatment: (a) 5 h; (b) 20 h; (c) 50 h; (d) 80 h; (e) 120 h; (f) 220 h; (g) 320 h.

provides a highly ordered mesostructured film, but the wall is amorphous.

The longer post-treatment brings the XRD peak shift to higher 2θ angles along with the degradation of the diffraction peak as shown in Figure 5. These show the vertical shrinkage of the periodic structure and the lowering of the ordering of the mesostructure. It should be emphasized that the peak after the 320-h post-treatment is still strong enough to prove the retention of the mesostructure though the intensity is considerably decreased. Because Figure 5 was obtained using the same sample film by repeating the XRD measurement and the corresponding vapor treatment, these data show that the mesostructure can be changed under relatively low temperature, even after a long period from the film deposition. When the relative humidity was lowered back to ~20% RH after a given post-treatment period, the changes in the XRD patterns were stopped.

As shown in Figure 6, the longer post-treatment caused variation also in the wide-angle diffraction pattern. Three broad peaks developed at $2\theta = 26°$, 33°, and 52°, and sharpened with the post-treatment time. Because these peaks can be assigned to the (110), (101), and (211) of cassiterite,[52] respectively, Figure 6 shows the development of the crystallization of SnO_2. The crystallization proceeded only when the film was held in the high-humidity atmosphere. When the amorphous film with the highly ordered mesostructure (e.g., after 5 h of post-treatment) was transferred into the low-humidity atmosphere (40 °C, 20% RH) again, the XRD peaks caused by cassiterite microcrystals were never observed, even after a very long period. Both of the XRD peaks due to the ordered mesostructure and microcrystals were never observed without the water-vapor post-treatment however long the accommodation in the dry atmosphere is.

The crystallization of the pore wall was also confirmed by electron diffraction (ED). The ED pattern of the film for the same region of the TEM image in Figure 4 A is shown in the inset (a) of Figure 4A. The concentric rings show the existence of the crystals. The lattice distances calculated from the observed diffraction pattern correspond to the lattice spacings of cassiterite.

From the broadening of the (211) diffraction peaks in Figure 6, the crystallite size in the films was calculated using the Scherrer formula. The changes of the calculated crystallite size and the intensity of the (100) diffraction peak of the hexagonal structure are shown in Figure 7. It was shown that the crystallization accompanies the degradation of the ordering of the mesostructure. A control experiment was performed without adding the surfactant in the precursor solution, but otherwise identical conditions. The change in the crystallite size in the surfactant-free film with the period of the post-treatment is also shown in Figure 7. It was shown that the existence of the surfactant scarcely affects the crystallization process in the present system, and the size of the final crystallite estimated by XRD was almost identical in both cases.

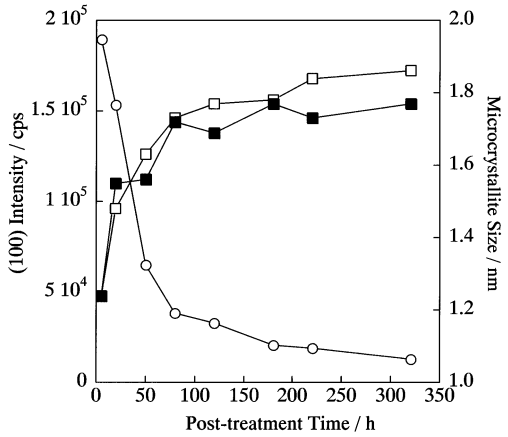

Figure 7. Change of the (100) diffraction peak intensity of the mesostructured tin oxide film with time of the water vapor post-treatment (○) and the corresponding change of the SnO_2 microcrystalline size (□). (■) Change of the SnO_2 crystal size in the SnO_2 film prepared without the surfactant. The crystal size was estimated from the broadening of (211) diffraction peaks using the Scherrer formula.

Effect of Water Contents in the Precursor Solutions. In this strategy, the post-treatment process undoubtedly includes hydrolysis. Therefore, it is likely that the film formation is affected by the water content in the reactant solution. The importance of water in the system has been pointed out for mesostructured zirconia[34] and titania.[35] However, in these reports, the distinction between the water in the precursor solution and vapor water has not been elucidated. In contrast to these reports, our results clearly show that water is not indispensable in the precursor solution to prepare the highly ordered mesostructured tin oxide film as long as the film undergoes the post-treatment with water vapor. To make the role of vapor water clearer, the effect of water added to the solution was investigated.

First, the influence of water in the alcoholic precursor solution was investigated. Water was added to the $C_{18}EO_{10}$ alcoholic solution with a molar ratio of H_2O/EtOH = 2.0/3.6. To this solution, the same amount of $SnCl_4$ was added with stirring. The solution was transparent and no change was seen by the eye by the addition of water. The substrate was coated with this solution and was subsequently dried under the conditions of 40 °C, 20% RH for 10 h. The obtained film was opaque and granular and provided only a broad weak XRD peak (trace (a) in Figure 8A). The addition of water in the precursor solution did not change the morphology and the structure of the film after the simple drying

(52) JCPDS #41-1445.

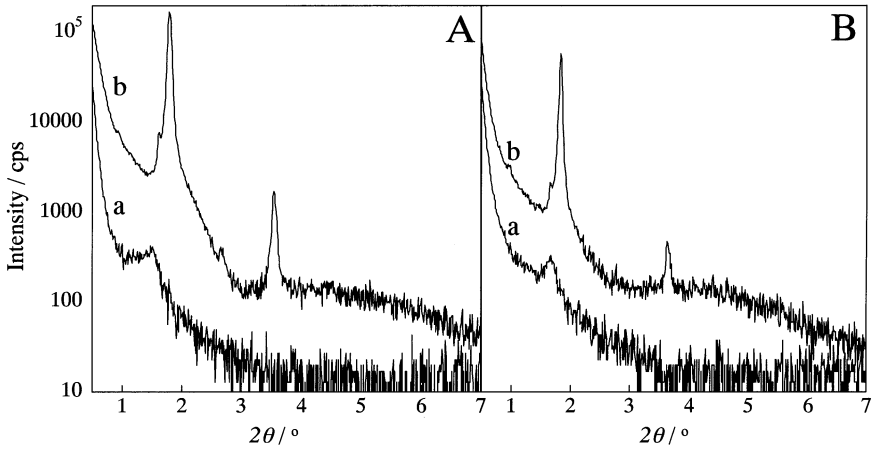

Figure 8. Changes of the XRD patterns of the mesostructured films by the water-vapor post-treatment. (A) The mesostructured film prepared from a $C_{18}EO_{10}$ water−ethanol mixture solution: (a) Before the post-treatment and (b) after the post-treatment. (B) The mesostructured film prepared from a $C_{16}EO_{20}$ aqueous solution: (a) Before the post-treatment and (b) after the post-treatment.

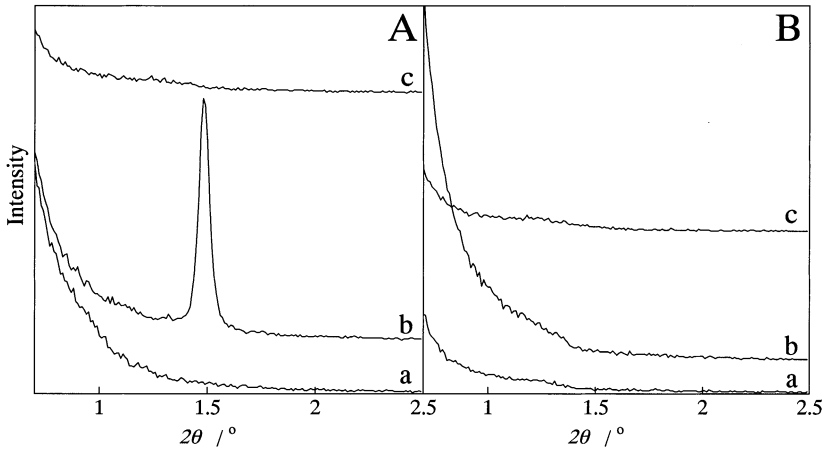

Figure 9. Changes of the XRD patterns during the drying process recorded for the films prepared from (A) aqueous solution and (B) ethanol solution: (a) 1 min; (b) 30 min; (c) 1 h of drying after the deposition.

process. The film after the drying process underwent the low-temperature post-treatment with water vapor under the conditions of 40 °C, 80% RH according to the same procedure employed for the water-free EtOH solvent case. The film turned transparent after a very short exposure to water vapor. The XRD pattern of the film after the 5-h post-treatment is shown as trace (b) in Figure 8A. The intense diffraction peaks caused by the highly ordered structure were observed after the post-treatment. The intensity of the main peak increased ∼400 times after the post-treatment. This behavior is identical to the one observed for the film prepared from the water-free alcoholic precursor solution. This proves that the water in the precursor solution does not affect the final mesostructured tin oxide film at all as long as the same conditions of the drying process and the post-treatment process are employed. It was also confirmed that the humidity during the dipcoating had no effect on the film structure for the conditions between ∼20% RH and ∼60% RH.

For further investigation of the effect of water in the precursor solution, the film formation was performed using an aqueous solution of tin tetrachloride and a surfactant instead of the alcoholic solution. Because the nonionic surfactant used for the alcoholic solution, $C_{18}EO_{10}$, has poor solubility in water, the same amount of $C_{16}EO_{20}$ was used instead. The aqueous solution of tin tetrachloride and the surfactant was transparent and no precipitation was observed. The substrate was coated with this aqueous solution and dried under the same conditions, 40 °C and 20% RH, for 10 h. The film after the drying process was opaque and granular just like the films prepared from the alcoholic solutions. The XRD pattern of the simply dried film from the aqueous solution is shown as trace (a) in Figure 8B. Even the film prepared from the aqueous solution provided no distinct mesostructure only by the simple drying process. The film prepared from the aqueous solution also turned transparent through the post-treatment, and the intense XRD peaks were observed after the 5-h exposure to water vapor (trace (b) in Figure 8B). The increase of the diffraction intensity of the main peak was ∼200 times.

The crystallization of the pore wall was observed in all the films after the long post-treatment, but never observed without the post-treatment regardless of the period of drying. It was shown that the supply of water from a vapor phase is indispensable for the crystallization of the pore wall.

The effect of water in the deposition solution was investigated not only for the final film structure but also for the transient structure during the drying process.

The XRD patterns of the films deposited from the aqueous and the alcoholic solutions after 1 min, 30 min, and 1 h of simple drying are shown in parts A and B, respectively, of Figure 9. Both of the films showed no regular structure after 1 min and 1 h of the drying process (traces (a) and (c)). However, a clear structural difference was observed between the two film samples after 30 min of the drying process (traces (b)); no substantial structural regularity was observed for the film prepared from the alcoholic solution, but on the other hand, a distinct diffraction peak was observed for the film prepared from the aqueous solution.

Discussion

Changes of the Surface Morphology through the Post-treatment. The opaque-to-transparent change of the film caused by the surface morphological change induced by water vapor proceeds very fast. As shown in Figure 3, the granular surface was almost flattened after only ~2 s. Such a fast macroscopic morphological change indicates the nonsolid property of the film in the early stages of the post-treatment. This property is caused by insufficient condensation of the wall-forming material, and the initial granular morphology indicates low viscosity of a nonpolymeric film. Several reports have described the flexibility of as-synthesized films with incomplete condensation of the inorganic species.[53,54]

However, not only condensation but also hydrolysis of the tin source can be considerably suppressed in the present opaque and granular films after the simple drying process regardless of the water content in the precursor solutions. This is confirmed by the experimental fact that the observed morphological change is independent of the water content in the precursor solutions. If only condensation is suppressed, the morphological change upon the water vapor post-treatment would not take place for the film prepared from the water-containing precursor solution because the condensation between the hydrolyzed species and consequent solidification could proceed in a dry atmosphere.

In the drying process, the solvents (ethanol and water) would evaporate rapidly to give the monomeric inorganic species containing considerably unhydrolyzed parts. When the films are moved to a high-humidity atmosphere, they gain fluidity by absorbing water from moisture, leading to the formation of smooth surface morphology.

Disordered Structure Formed through the Simple Drying Process. The films simply dried under low-humidity conditions showed only poor structural regularity (Figure 2 (a), Figure 8A,B (a)). This is inconsistent with the conventional solvent-evaporation process in which a highly ordered mesostructure can be formed just after the film formation. The fact that an ordered structure was not obtained by the simple solvent evaporation process shows either that the ordered structure was not formed or that the ordered structure was formed once and then ruined.

When $SnCl_4$ is dissolved in an alcoholic solution, the partial ligand exchange takes place according to following formula (A).[55] Although water from moisture would produce a small amount of partially hydrolyzed species, the tin source is mainly in an unhydrolyzed state. On the other hand, the surfactant dissolved in the alcoholic solution does not form ordered structures of liquid-crystal phases.

$$SnCl_4 + xROH \rightarrow SnCl_{4-x}(OR)_x + xHCl \quad (A)$$

When water is added to the system, partial hydrolysis is expected to take place according to formula (B).[55] However, in this system, condensation of the partially hydrolyzed species would be hindered by the existence of a large amount of chlorine.[55,56] The surfactant cannot form an ordered liquid-crystal phase because of the large amount of alcohol. Although selective evaporation of ethanol during the evaporation process may lead to the formation of an ordered lyotropic liquid-crystal phase, the structure will be ruined by further evaporation of water before the condensation of wall-forming materials as will be discussed later. For these reasons, a highly ordered mesostructure was not obtained by the simple drying process, even though water was added in the reactant solution (Figure 8A (a)).

$$SnCl_{4-x}(OR)_x + yH_2O \rightarrow SnCl_{4-x}(OR)_{x-y}(OH)_y + yROH \quad (B)$$

When alcohol was used as a main solvent, the films simply dried under low-humidity conditions would be a disordered mixture of the surfactant and the monomeric tin compounds that had undergone partial hydrolysis. The broad XRD patterns show the existence of some structural ordering in the films after a simple drying process. However, the peak is too broad and weak to elucidate the structure.

The rapid hydrolysis of $SnCl_4$ does not take place, even when water is used as a solvent instead of ethanol. $SnCl_4$ is soluble in water and definite hydrates such as $SnCl_4 \cdot 5H_2O$ can be isolated from the aqueous solution.[57] The rate of hydrolysis of $SnCl_4$ in the aqueous solution is low because of the existence of excess Cl^-, and equilibrium is attained before the hydrolysis is complete.[58] Therefore, when the film was prepared using an aqueous solution of $SnCl_4$ and the surfactant, the inorganic species would exist mainly in monomeric states, at most, with a very few oligomeric components after simple drying under low-humidity conditions. On the other hand, the surfactant would form ordered structures based on the corresponding lyotropic liquid-crystal phase unless the inorganic component prevents the formation. However, as shown in trace (a) in Figure 8B, the ordered mesostructure has not been obtained through a simple drying process. This is explained by the rapid evaporation of water and slow condensation

(53) Soler-Illia, G. J. A. A.; Louis, A.; Sanchez, C. *Chem. Mater.* **2002**, *14*, 750.
(54) Brinker, C. J.; Lu, Y.; Sellinger, A.; Fan, H. *Adv. Mater.* **1999**, *11*, 579.
(55) Epifani, M.; Alvisi, M.; Mirenghi, L.; Leo, G.; Siciliano, P.; Vasanelli, L. *J. Am. Ceram. Soc.* **2001**, *84*, 48.
(56) Manorama, S. V.; Reddy, C. V. G.; Rao, V. J. *Nanostruct. Mater.* **1999**, *11*, 643.
(57) Greenwood, N. N.; Earnshaw, A. *Chemistry of the Elements*, 2nd ed.; Butterworth-Heinemann: Oxford, 1997.
(58) Mellor, J. W. *A Comprehensive Treatise on Inorganic and Theoretical Chemistry*; Longmans, Green and Co. Ltd.: London, 1952; Vol. 7.

of the inorganic species. That is, the ordered structure corresponding to the lyotropic liquid crystal-phase formed during the drying process was lost before fixing the inorganic framework through condensation because the water content became too low to form the lyotropic liquid-crystal phase.

This hypothesis was confirmed by the in situ XRD experiments. For the film prepared from the aqueous solution, a sharp XRD peak corresponding to an ordered structure was once observed during the drying process, but it disappeared with the completion of the drying process (Figure 9A). On the other hand, no transient XRD peak was observed for the film prepared from the alcoholic solution (Figure 9B).

Formation of Highly Ordered Mesostructure by the Water Vapor Post-treatment. Every film with disordered structure obtained through the simple drying process shows the structural change to a highly ordered hexagonal structure by exposure to water vapor. The structural change seems independent of the solvent in the reactant solution. Because the structural change accompanies the morphological change, it is clear that the water vapor brings about a whole structural rearrangement. In the rearrangement, two elemental phenomena are obviously included. One is the formation of the ordered lyotropic liquid-crystal phase and the other is proceeding of hydrolysis and condensation of the inorganic species. The cooperation of these two phenomena leads to the solidification of the highly ordered structure.

When the disordered film after the simple drying process is put into a high-humidity atmosphere, the film absorbs water rapidly, and consequently, the lyotropic liquid-crystal phase that is determined by the water content and the temperature is formed. This rearrangement can take place because of the monomeric properties of the inorganic species in the disordered films. At the same time, hydrolysis of the inorganic species proceeds because the generated HCl can be removed into the vapor phase. This is evidenced by the fact that HCl is generated during the water vapor treatment. During the proceeding of the hydrolysis, the concomitant condensation leads to the formation of polymeric Sn−O−Sn species. Since the inorganic wall in the mesostructured film is fixed after the appropriate water vapor post-treatment, the following drying process does not result in further structural change in the film.

In this strategy, the formation of the lyotropic liquid-crystal phase that provides the ordered mesostructured SnO_2 film is caused by the absorption of water from the gas phase. This vapor-induced liquid-crystal templating is advantageous compared with the conventional solvent evaporation process for several reasons. One advantage is the higher ordering of the mesostructure; the longer time for rearrangement allows improved ordering in the formed lyotropic liquid-crystal phase. This is proved by the TEM image shown in Figure 4A. To the best of our knowledge, this is the first TEM image of a non-siliceous mesostructured material film that proves the formation of a highly ordered channel structure over the whole film thickness. Another advantage is the high reproducibility of the formed mesostructure; the final structure is affected by neither the water content in the precursor solution nor the conditions of the coating atmosphere such as humidity and temperature. The needlessness of strict control of the coating conditions is favorable for industrial applications.

Crystallization of the Pore Wall. As shown in Figure 6, the long vapor post-treatment induced the crystallization of SnO_2. Although the preservation of the mesostructure upon post-treatment is shown by XRD (Figure 5), the possibility that the crystallization selectively took place in the partially collapsed part of the film cannot be excluded. However, Figure 4A clearly shows the coexistence of the highly ordered mesostructure and the microcrystalline SnO_2. The confirmation of the microcrystals by XRD excludes the possible crystallization by an electron beam. To the best of our knowledge, this is the first report that proves the crystallization of the pore wall with the complete exclusion of the possibility of partial collapse of the highly ordered mesostructure.

As discussed above, it was shown that the high structural ordering of the mesostructured SnO_2 film was preserved upon the crystallization of the pore wall. However, as shown in Figure 7, the ordering of the mesostructure decreases with the progress of the crystallization. This is expected due to the stress caused by the volume change upon crystallization.

The growth of the SnO_2 crystals tends to terminate when the crystal size estimated by XRD approaches ~2.0 nm. This crystallite size is smaller than the thickness of the pore wall estimated by STEM, which is consistent with the preservation of the mesostructure. The crystallite size is not suppressed by the wall thickness, as is shown by the control experiment without using the surfactant. The size of the crystallites in the films should be determined by the density of the nucleation sites. Therefore, the present results would show that the nucleation density was high enough in each case, and consequently, the suppression of the crystal growth by the dimensions of the porous structure was not observed. The inherent suppression of the crystal growth[56] in the present SnO_2 formation process should allow the observed retention of the highly ordered mesostructure. However, the Sherrer formula can lead to underestimation of the average crystallite size because the contribution of smaller size components in a crystallite-size distribution dominates the broadening of the diffraction peaks. For this reason, the actual crystallite size might be larger than that estimated by XRD.

The crystallization of the wall is observed only when the film is held in the high-humidity atmosphere for a considerably long period. When the film was transferred into a low-humidity atmosphere after the relatively short post-treatmment, the crystallization of the pore wall as well as the degradation of the mesostructure has never been observed. There would be two explanations for this. One is the insufficient hydrolysis of the tin source in the film, and the other is the direct involvement of water for crystallization. The elucidation of the detailed mechanism of the observed crystallization, including the role of water, is the next step in our study.

Conclusion

An optically transparent mesostructured tin oxide film with highly ordered hexagonal structure and micro-

crystalline pore wall was prepared by coating a substrate with a precursor solution containing tin tetrachloride and a nonionic surfactant followed by a post-treatment with water vapor. The ordered mesostructure was formed through the formation of a lyotropic liquid-crystal phase that is induced by water vapor, and the monomeric properties of the tin source in the as-prepared film make the macroscopic and mesoscopic rearrangements possible. The vapor-induced lyotropic liquid-crystal templating method is applicable for various materials by controlling hydrolysis and condensation. The present mesostructured tin oxide film containing microcrystals is promising for electronic applications. The use of surfactants with functional groups or functional guest species that can be directly introduced into the micelle structure will lead to the formation of new electronic materials through a marvelous self-organization process.

Acknowledgment. The authors acknowledge Professor K. Kuroda at Waseda University for helpful discussions. The authors also acknowledge Dr. K. Inaba (Rigaku Co. X-ray Research Laboratory) for the in-plane X-ray diffraction measurements.

Supporting Information Available: Figure of a scanning profile (in-plane XRD) for a mesostructured tin oxide film (PDF). This material is available free of charge via the Internet at http://pubs.acs.org.

CM020870A